Digestive Diseases and Sciences, Vol. 42, No. 7 (July 1997), pp. 1331–1343

REVIEW ARTICLE

What Can Be Measured from Surface Electrogastrography

Computer Simulations

JIE LIANG, MS and J.D.Z. CHEN, PhD

The aims of this study were to investigate the detectability of the propagation of the gastric slow wave from the cutaneous electrogastrogram (EGG) and the patterns of the EGG when the gastric slow waves are uncoupled. A mathematical model was established based on the volume conductor theory to simulate the transfer of the serosal gastric slow wave from the stomach to the abdominal surface. A number of computer simulations were conducted using the model, and the periodic cross-correlation function was used to estimate the phase shift between the four channels. It was found that the propagation of the gastric slow wave was detectable from the multichannel EGG signals. The detectability of the propagation was, however, associated with a number of factors, such as the thickness of the abdominal wall and the propagation velocity of the serosal slow wave. The amplitude of the EGG was found to be associated with the coupling/uncoupling and propagation velocity of the gastric slow wave. The amplitude of the EGG increased when the propagation velocity of the gastric slow wave increased. The amplitude of the EGG was substantially decreased when the gastric slow waves were uncoupled. The uncoupling of the gastric slow wave at a frequency of 3 cpm produced dysrhythmias in the EGG, including tachygastria, bradygastria, and arrhythmia. The power spectra of simulated different positional EGG signals showed similar patterns when the gastric slow wave was coupled and different and unpredictable patterns when the gastric slow wave was uncoupled. In conclusion, multichannel EGG recordings may be necessary to obtain more information on gastric slow waves from the abdominal electrodes. The propagation and coupling or uncoupling of the gastric slow wave may be detected from multichannel EGG recordings.

KEY WORDS: electrogastrography; mathematical model; computer simulation; gastrointestinal motility; gastric emptying.

Electrogastrogram (EGG), a cutaneous measurement of gastric electrical activity, has long been studied (1), and research results showed great clinical potentials for the EGG (2–9). Improved measurement and analysis of the EGG have made it more accurate in reflecting the corresponding gastric electrical activity (GEA) of the stomach. Efforts have been made to simultaneously measure both the serosal GEA and the cutaneous EGG signals for the validation of the EGG (10–12). Investigators continue to try to extract more information from the noninvasive EGG.

GEA at different locations of the stomach has different waveforms, phases, and amplitudes. For a healthy stomach, it propagates from the corpus to the pylorus with an increasing amplitude and velocity (13). In this case, the phase, amplitude, and frequency of the GEA are regularly transferred from point to point. This phenomenon is called "coupling." In un-

Manuscript received September 6, 1996; revised manuscript received February 2, 1997; accepted April 11, 1997.

From the Lynn Institute for Healthcare Research, Integris Baptist Medical Center, Inc., Oklahoma City, Oklahoma.

Address for reprint requests: J.D.Z. Chen, Lynn Institute for Healthcare Research, Integris Baptist Medical Center, Inc., 3300 Northwest Expressway, Oklahoma City, Oklahoma 73112.

coupled cases (11, 14), the propagation no longer exists, and the phase, amplitude, and frequency show largely irregular behavior. These phenomena may be reflected in the cutaneous EGG recordings, but it is unknown how these are reflected in the EGG.

If the abdominal wall is regarded as an input–output system, then the input of the system is serosal GEA signals and the output is cutaneous EGG signals. In the real case, both the input and output are functions of time and space. In order to extract more information about the input, multiple points at the output need to be studied. This is a kind of multiinput–multioutput system. A mathematical model may be established to simulate such a system.

With a few exceptions (15, 16), cutaneous EGG recordings have been performed with only one channel recorded and/or analyzed. This method may lose useful information about GEA, such as the propagation of GEA and the coupling/uncoupling of GEA. Intuitively, a multichannel recorder would be expected to provide more information. In this paper, a mathematical model was established to approximate the transfer of GEA from the stomach to the abdomen. Computer simulations were performed to simulate serosal GEA signals and multichannel cutaneous EGG signals based on this model. The aims of this study were to investigate the detectability of the propagation of GEA from the EGG and the pattern of the EGG when GEA is uncoupled.

SIMULATION OF SEROSAL SLOW WAVES

There are two kinds of electric activity in the stomach: slow waves, which are omnipresent periodic potentials, and contraction-related second potentials, with or without spikes (17). The latter was assumed absent since the aim of this study was to investigate the transfer of the slow wave from the stomach to the abdomen.

The frequency of the gastric slow wave in the canine stomach is about 5 cycles/min (cpm). It propagates from the corpus to the pylorus with an increasing amplitude and velocity. The maximum amplitude is about 0–1 mV in the corpus and 2–3 mV in the antrum. The propagation velocity is about 0.1–0.2 cm/sec in the orad corpus and 1.5–4.0 cm/sec in the antrum (18). The total phase lag from the originating point in the corpus to the pylorus is about three cycles. Sarna stated that the longitudinal phase lag is around 70–100°/cm near the most proximal site and around 8–20°/cm near the pylorus in different dogs (19).

The gastric slow waves in humans are similar to those in dogs. Their frequency is about 3 cpm. The average phase lags are 70°/cm high in the corpus and 25°/cm in the terminal antrum (20).

For the simulation of the transfer of the slow waves from the stomach to the abdomen, we assumed that the stomach was cylindrical and all slow waves concentrated in one vertical line, propagating from the top, corresponding to the pacemaker of the slow waves in the corpus, to the bottom, corresponding to the pylorus. The circumferential propagation was ignored.

The serosal slow waves were simulated as follows: the first portion of the slow waves was assumed to be a rectified sinusoid with an adjustable duration followed by a flat line. The amplitude increased logarithmically or exponentially, and the propagation velocity increased linearly (logarithmic phase shift) or remained fixed from the corpus to the pylorus. The total phase shift between the most proximal and distal slow waves in the simulations varied from 1 to 3 cycles (or 20 to 60 sec).

Figure 1 presents one of typical patterns of simulated serosal slow waves. The numbers 1 to 10 stand for different positions in the stomach with 1 referring to the originating point of the slow wave, 5 to the junction between the corpus and the antrum, and 10 to the pylorus. The frequency of the slow waves was 3 cpm and the rectified sinusoid had a duration of 2.4 sec.

MATHEMATICAL MODELING OF THE EGG

The EGG at a certain point on the abdomen is a summation of the contributions of all internal gastric activities to that point. In order to simulate the EGG, we first discuss the relevant electrical properties of the biological materials and their effects.

The propagation of the electric activity in the smooth muscle results from the depolarizing effect of action currents on surrounding resting membranes. When a membrane is activated, the current density is strongest in the immediate vicinity, but there will be current everywhere in the surrounding medium.

Assume the medium is linear, homogenous, isotropic, and characterized by physical parameters, $\tilde{\mu}$, $\tilde{\sigma}$ and ξ, the potential φ at point (x', y', z') due to a volume current source density I_v (x, y, z) can be calculated according to the following formula (21):

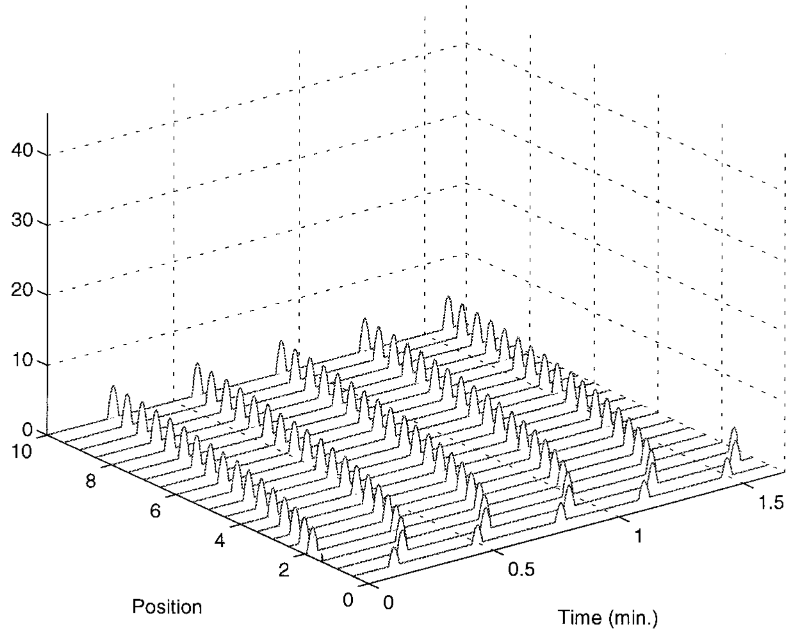

Fig 1. Simulated gastric slow waves on the serosa of the stomach. Position 1 corresponds to the pacemaker site, and position 10 corresponds to the pylorus. The frequency of the simulated slow wave was 3 cpm. The propagation velocity increased linearly, and the amplitude of the slow wave increased logarithmically from the corpus to the pylorus.

$$\varphi(x', y', z') = \frac{1}{4\pi(\tilde{\sigma} + i\omega\xi)} \int \frac{I_v(x, y, z)e^{-\mathrm{ikr}}}{\mathrm{r}} \mathrm{dv} \qquad (1)$$

and

$$k^2 = -i\omega\tilde{\mu}\tilde{\sigma}\left(1 + \frac{i\omega\xi}{\sigma}\right) \qquad (2)$$

where, $\tilde{\mu}$ is permeability, $\tilde{\sigma}$ is conductivity, ξ is dielectric constant, $i = (-1)^{-1/2}$, and ω is angular frequency. r is the distance between the source point and the field point:

$$r^2 = (x - x')^2 + (y - y')^2 + (z - z')^2 \qquad (3)$$

The unprimed variables refer to the source point in the stomach, the primed variables to the field point on the abdomen.

According to the electrical properties of biological material (22–24), the ratio of displacement to conduction current

$$\frac{i\omega\xi}{\tilde{\sigma}} \ll 1 \qquad (4)$$

that is,

$$\tilde{\sigma} + i\omega\xi \doteq \sigma \qquad (5)$$

The term e^{-ikr} in equation 1 represents the phase delay, the time required for changes at the source to "propagate" to a field point. It can be written as:

$$e^{-\mathrm{ikr}} = 1 - \mathrm{ikr} - \frac{(\mathrm{kr})^2}{2!} - \mathrm{i}\frac{(\mathrm{kr})^3}{3!} + \cdots \qquad (6)$$

The mean conductivity values for blood, lung, liver, fat, and human trunk are 0.67, 0.05, 0.14, 0.04, and 0.21, respectively (6–8), from which we see that the conductivity of fat is low. Since the media for the propagation of slow waves from the serosa of the stomach to the abdominal skin is mainly fat and human trunk, we choose an average value of 0.125.

Because of the absence of magnetic materials in the media, the permeability, $\tilde{\mu}$, is the free space value of $4\pi \times 10^{-7}$ henry/m. The maximum distance $r_{\max}$ between the stomach and the abdomen is less than 0.5 m.

According to the above values of $\tilde{\mu}$, $\tilde{\sigma}$, and $r_{\max}$, we have

$$kr = \sqrt{-i\omega\tilde{\mu}\tilde{\sigma}\left(1 + \frac{i\omega\xi}{\tilde{\sigma}}\right)}\, r < 0.00157(1 - i) \qquad (7)$$

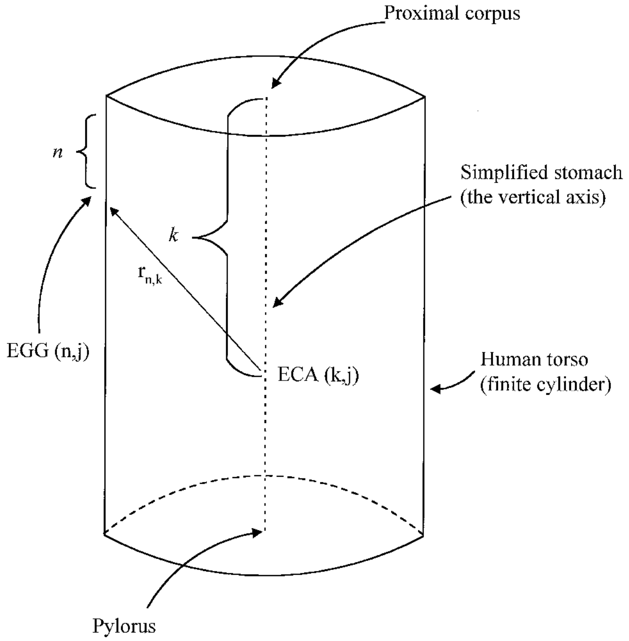

Fig 2. Simplified representation of human torso and stomach. The torso is simplified as a cylinder, and the stomach is simplified as the vertical axis.

where the value $[1 + (i\omega\xi)/\tilde{\sigma}]$ is conservatively set to be 2 and e^{-irk} is set to be 1 and $\omega_{\max}$, $2\pi \times 10$ since the highest frequency component of the gastric signal is less than 10 Hz.

Finally, the potential at field points (x, y, z) (equation 1) can be simplified as

$$\varphi(x', y', z') = \frac{1}{4\pi\tilde{\sigma}} \int_v \frac{I_v(x, y, z)}{r} dv \tag{8}$$

Now assume there exist M current sources along the vertical axis of the stomach and these current sources are simulated gastric slow waves shown in Figure 1. Denote the kth serosal gastric signal at discrete time j as $ECA(k, j)$ and the nth cutaneous gastric signal as $EGG(n, j)$ (Figure 2); then we have

$$EGG(n, j) = b \sum_{k=1}^{M} \frac{ECA(k, j)}{r_{n,k}}, \tag{9}$$

where b is a constant factor, $r_{n,k}$ is the distance between the measure point on the abdomen and the kth internal source signal. $r_{n,k}$ is associated with the distance between the stomach and the abdomen and with the size of the stomach. From the above equation, we see that the cutaneous EGG is a weighted summation of internal gastric activities.

SIMULATION RESULTS

Computer simulations were performed to investigate which factors affect the cutaneous EGG signals and to investigate the detectability of the propagation of the gastric slow waves from multichannel EGG recordings. In this paper, four-channel EGG recordings were simulated. Two of them corresponded to the abdominal points right above the corpus and pylorus, and the other two were evenly placed in between. All simulations were performed on an IBM PC 486 in C++ language and MATLAB. The periodic cross-correlation functions between the four-channel simulated cutaneous EGG signals were used to detect the phase shift among them.

Detectability of Propagation of Slow Waves from EGG

Generally speaking, the propagation of the gastric slow waves is detectable according to the simulation results. Phase-shifts were observed from simulated multichannel cutaneous EGG recordings (Figure 3). However, the detectability of the propagation of the gastric slow waves was found to be associated with a few factors described in the following:

1. Observability Factor γ. The observability factor γ is defined as the ratio between the length of the stomach and the thickness of the abdominal wall. The thinner the abdominal wall, the better the observability is. This means that the detection of the phase shift is more difficult for obese subjects. Figure 4 presents the relationship between the total phase-shift observable from the multichannel EGG signals and the observability factor γ. It is seen that the observable total phase shift is approximately exponentially correlated with the observability factor. The total phase-shift for $\gamma = 10$ and 5 was 7.5 and 2.1 sec, respectively. The phase shift was not detectable when $\gamma = 1$ or smaller, in which case the thickness of the abdominal wall is equal to or greater than the longitudinal length of the stomach.

2. Width of Slow Wave. The width of the first portion (rectified sinusoid) of the slow waves measured serosally is often different for different subjects. Typically, it is about 3–5 sec. In our simulations, two extreme situations were tested. One of the widths was set to 2.67 sec, while the other was set to 5.33 sec. The results showed that it did not make any difference in

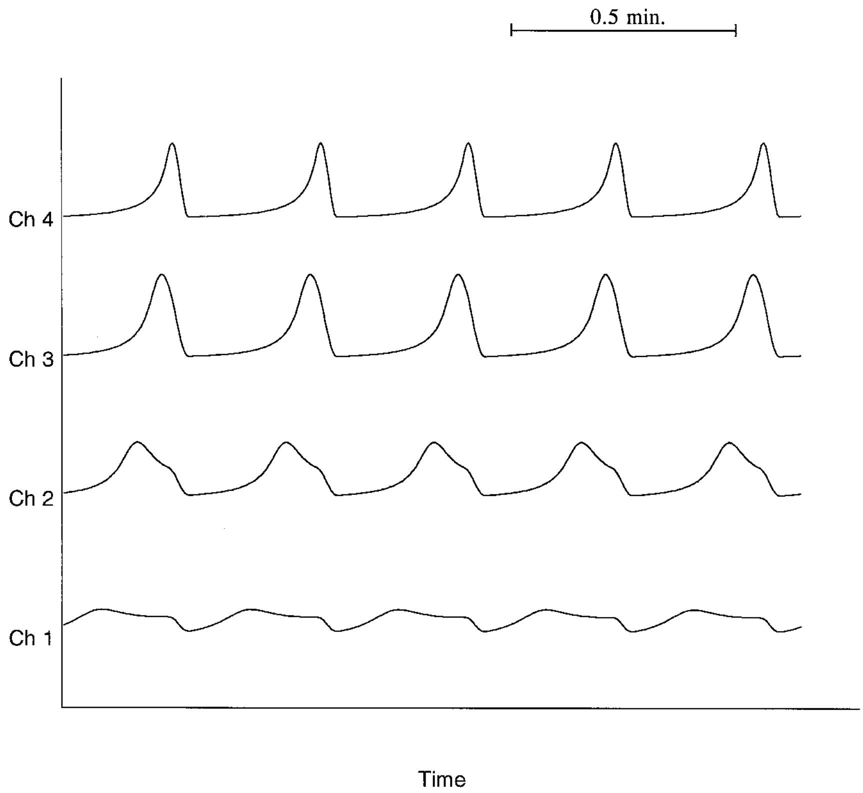

Fig 3. Simulated cutaneous EGG signals. Channel 1 corresponds to the EGG above the proximal corpus, and channel 4 corresponds to the EGG above the pylorus. The EGG signals were generated using the simulated serosal slow waves presented in Figure 1 based on the mathematical model with an observability factor of $\gamma = 10$. It is seen that the amplitude is lowest in channel 1 and highest in channel 3. The propagation of the slow wave from channel 1 to channel 4 is observed.

the observability of the gastric slow wave when the width was doubled from 2.67 to 5.33 sec. Therefore, the width of the slow waves within certain ranges hardly affects the phase-shift information in the multichannel cutaneous EGG recordings.

3. Total Phase Lag of Serosal Slow Wave. The total phase lag of the serosal slow wave from the corpus to the pylorus plays an important role in the detection of the propagation from the multichannel cutaneous EGG recordings. The phase shift between the channels became large when the total phase lag of the serosal slow wave was large and small when the total phase lag of the serosal slow wave was small. This is intuitively reasonable. The simulation results showed that the total phase shift in the multichannel cutaneous EGG signals decreased from 7.5 to 2.9 sec when the total phase lag of the serosal slow wave from the corpus to the pylorus decreased from $3 \times 360°$ (1 min) to $360°$ (20 sec). In addition, an increase of the amplitude of the simulated cutaneous EGG was observed when the propagation velocity of the serosal slow wave increased (the total phase lag decreased). The simulation results are shown in Figure 5. It is seen that the amplitude of the simulated EGG increased when the total phase lag of the serosal slow wave decreased from $3 \times 360°$ to $360°$, but meanwhile the energy (area under the curve) of the EGG signal remained unchanged.

4. Propagation Velocity. Based on the real recordings (25), the propagation velocity of the serosal slow waves varied from person to person. There is no single mathematical expression that could be used to model all different propagations. In simulations, constant or linearly increased propagation velocities were simulated, which were extreme cases. In real cases, the propagation velocity is mostly somewhere in between. The phase-shift between the four-channel cutaneous EGG signals was smaller (the total phase shift was 4.5 sec) for the constant propagation velocity than that for the linearly increased propagation velocity (the total phase shift was 7.5 sec).

5. Noise and Low-Pass Filtering. Noise always ex-

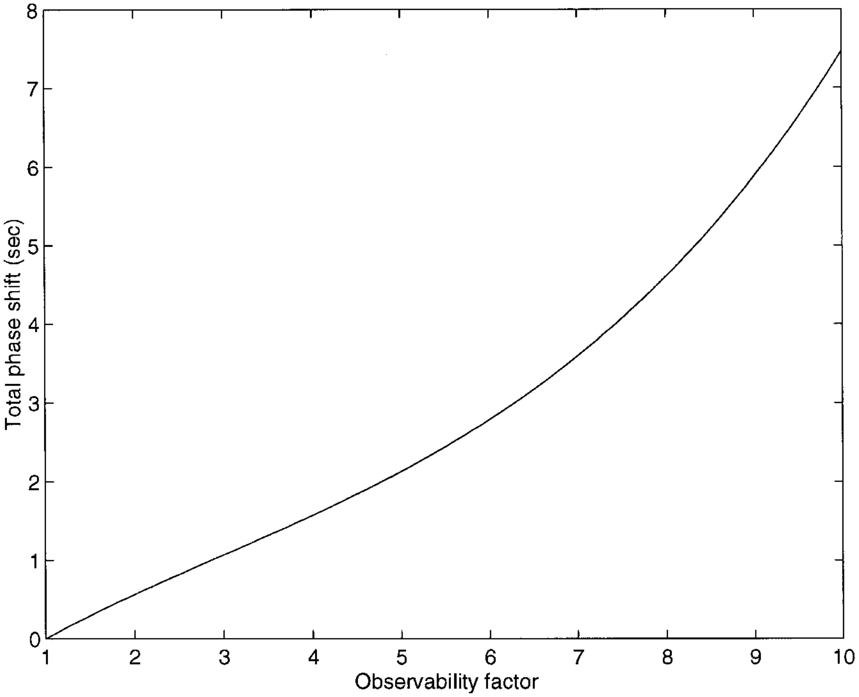

Fig 4. Effects of the observability factor γ on the detectability of the slow wave propagation. The total phase shift observed between EGG signals in channel 1 and channel 4 was approximately exponentially correlated with the observability factor γ. The simulated γ values were 1, 3, 5, and 10. The curve was obtained using the cubic spline interpolation.

ists in real EGG signals. There are different noises in cutaneous EGG recordings. The sources of the noises include the electrocardiogram (ECG), respiration, and motion artifacts. To simulate these noises, Gaussian noise was added to the simulated EGG signals (Figure 6A). Simulations were performed to determine the effect of low-pass filtering on the detectability of the slow wave propagation. The simulation was performed 20 times by adding Gaussian noise to the simulated cutaneous EGG signals. The mean values and the standard deviations of the noise were the same for the four channels, but the signal-to-noise ratios of the four-channel EGG signals were different. This was because the energies of the EGG signals of the four channels were different. The low-pass filter used was a fifth-order Butterworth type, and the cutoff frequency was 0.23 Hz. It was found that low-pass filtering statistically improved the performance of the phase-shift detection in the EGG signals. As shown in Table 1, the filtered (or denoised) EGG signals led to more accurate mean values of the phase shifts (closer to those obtained from the clean EGG data) and smaller standard deviations than the unfiltered noisy EGG signals. Filtered EGG signals are presented in Figure 6B.

Effects of Uncoupling of Slow Waves on EGG

All computer simulations described above were performed under the condition of coupling, ie, gastric slow waves propagated from the corpus to the pylorus. Under this condition, all cutaneous EGG signals revealed a dominant frequency of 3 cpm. Figure 7 presents the power spectra of the four-channel cutaneous EGGs simulated under the condition of coupling. It is seen that the dominant frequency of the EGG was 3 cpm in all four channels. It can also be observed that the power of the EGG at 3 cpm was lower in channels 1 and 4 and higher in channels 2 and 3. The simulated EGG above the distal antrum (channel 3) had the highest power at the frequency of 3 cpm.

1. Complete Uncoupling. In this case, all serosal slow waves had a frequency of 3 cpm. However, they did not propagate from the corpus to the pylorus, and their phases were random. The random phases of the simulated serosal slow waves were generated by a Gaussian-distributed random signal. The simulation results showed that the dominant frequency of the simulated EGG signals was not at 3 cpm but rather random and unpredictable, as shown in Figures 8 and

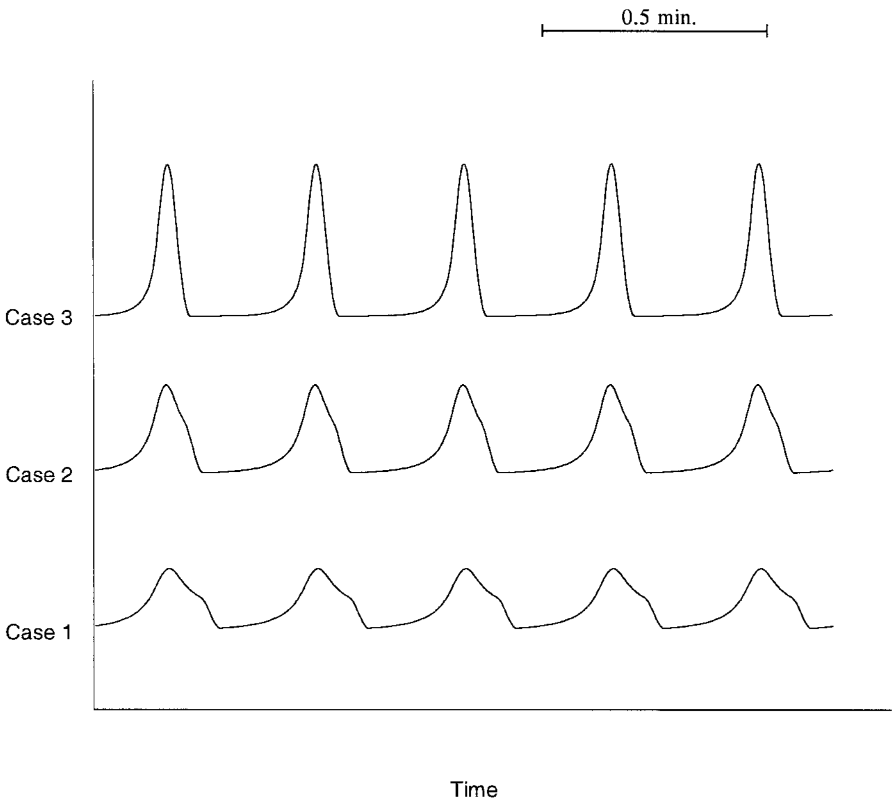

Fig 5. Cutaneous EGG signals of channel 2 simulated with different propagation velocities of the gastric slow wave. The EGG signals presented in cases 1–3 were obtained with a total phase lag of the serosal slow waves of 360°, 720°, or 1080°, respectively. The amplitude of the EGG increased when the propagation velocity of the gastric slow wave increased (the total phase lag decreased), but the energy (area under the curves) of the EGG remained unchanged.

9. Figure 8 presents the power spectra of the four-channel EGG signals simulated under the condition of complete uncoupling. It was observed that four different positional EGG signals had different power spectra. As shown in Figure 8, the EGG showed dominant bradygastria (frequency below 3 cpm) and secondary tachygastria (frequency above 3 cpm) in channel 1, dominant tachygastria and secondary bradygastria in channel 2, a combination of 3 cpm and multiple tachygastrias in channel 3, and dominant 3 cpm in channel 4. This was not a fixed pattern, however. The power spectrum of the simulated EGG at a fixed location varied under different simulations. Figure 9 shows the power spectrum of the EGG signals in channel 2 obtained in four different simulations. The change of the power spectrum of the EGG under different simulations was very obvious. The EGG signals under these different simulations had different components. Numerous computer simulations have shown that uncoupling can generate bradygastria, tachygastria, or the coexistence of bradygastria and tachygastria from uncoupled 3 cpm serosal slow waves. This phenomenon was different from the traditional concept that tachygastria or bradygastria in the cutaneous EGG is caused only by tachygastria or bradygastria in the serosal GEA signals.

2. Semiuncoupling. In real disease situations, the propagation of the gastric slow wave may be impaired but not completely, which may be called semiuncoupling. Two semiuncoupling cases were simulated. In the first case, the phase shift of the upper stomach was coupled, whereas that of the distal stomach was not coupled and random. In this case, the EGG signals in channels 1 and 2 were relatively normal. A phase shift of 1.6 sec was observed between EGG signals in channels 1 and 2 under the condition that the propagation velocity of the serosal slow wave increased linearly. In the second case, the proximal stomach was uncoupled, and the distal stomach was coupled with a linearly increasing propagation velocity. In that case, the EGG signals in channels 3 and 4 showed normal 3 cpm slow waves. The phase shift

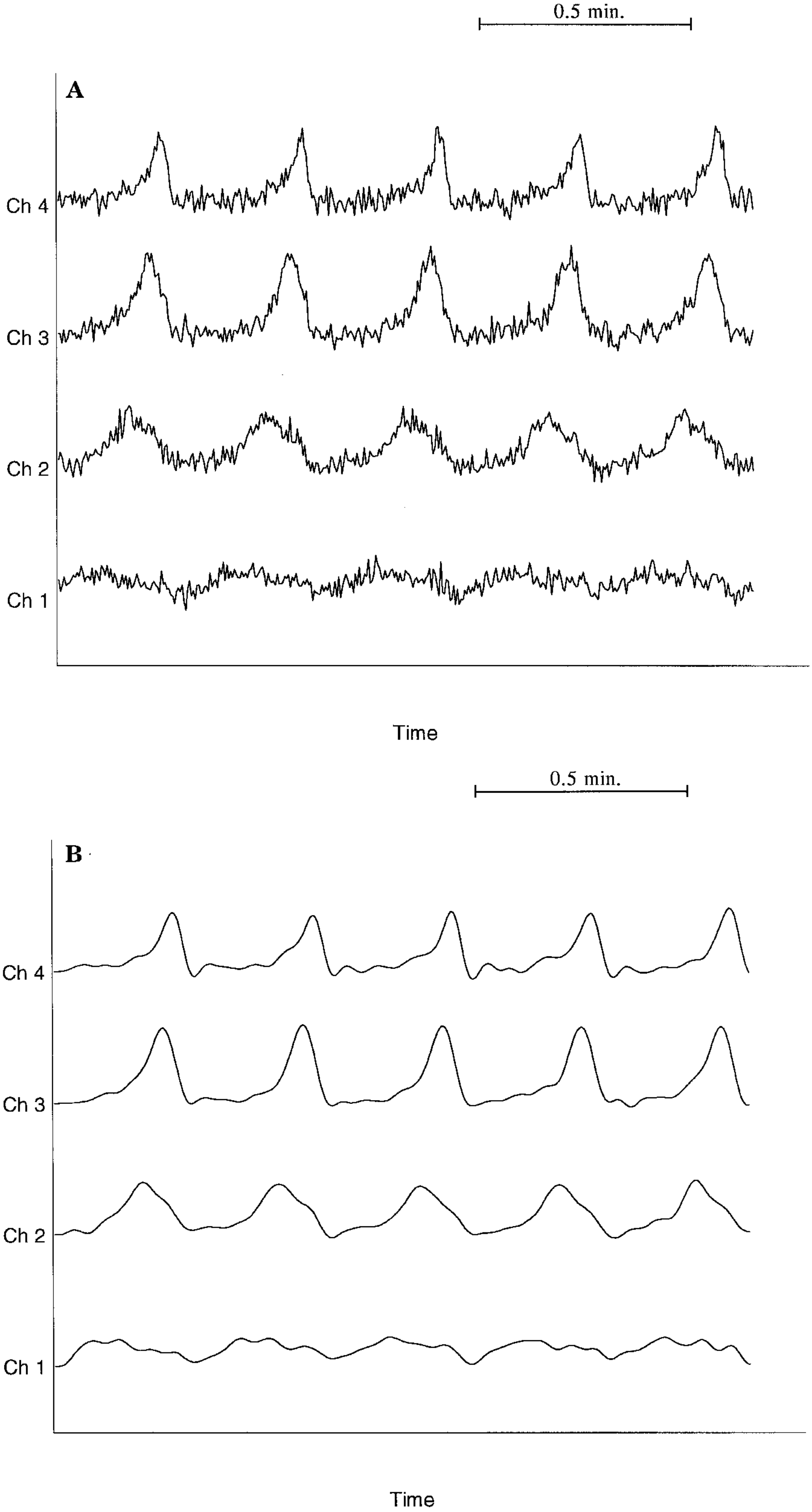

Fig 6. (A) Simulated cutaneous EGG signals with additive Gaussian noise. (B) The EGG signals after filtering with a fifth-order low-pass Butterworth filter with a cutoff frequency of 0.23 Hz.

TABLE 1. PHASE SHIFTS*

	Channel			
	1 & 2	*2 & 3*	*3 & 4*	*Total*
Clean data	3.73	2.67	1.07	7.47
Noisy data	3.73 (±0.91)	2.47 (±0.29)	1.11 (±0.15)	6.95 (±0.93)
Denoised data	3.57 (±0.67)	2.56 (±0.24)	1.08 (±0.06)	7.22 (±0.70)

*Mean values and standard deviations; measured from the simulated EGG signals without noise, with noise, and with noise and low-pass filtering. The signal-to-noise ratios (mean values and standard deviations) for channels 1–4 were −0.45 (±0.41), 7.86 (±0.34), 11.16 (±0.31), and 8.87 (±0.41) dB, respectively. The cutoff frequency of the fifth-order Butterworth filter was 0.23 Hz.

between EGG signals in channels 1 and 2 disappeared. The phase shift between channels 2 and 3 reduce to half, whereas the phase shift between channels 3 and 4 remained unchanged; ie, the same as in the coupled situation.

DISCUSSION

In this paper, the serosal gastric slow waves were simulated, a computer mathematical model was established for the transfer of the serosal gastric slow wave from the stomach to the abdominal surface, and computer simulations were conducted to investigate the detectability of the propagation of the gastric slow wave from the EGG and the effect of uncoupling on the cutaneous EGG.

Since the first measurement of the EGG, many efforts have been made in exploring clinical applications of electrogastrography. A number of recent papers have shown great diagnostic potentials of the EGG in clinical gastroenterology (2–9, 26–29). Mathematical models have been common and successful in biomedical research, such as in electrocardiography and electrical conduction studies in active nerve fibers. Once a mathematical model is established, computer simulations can be conducted to simulate

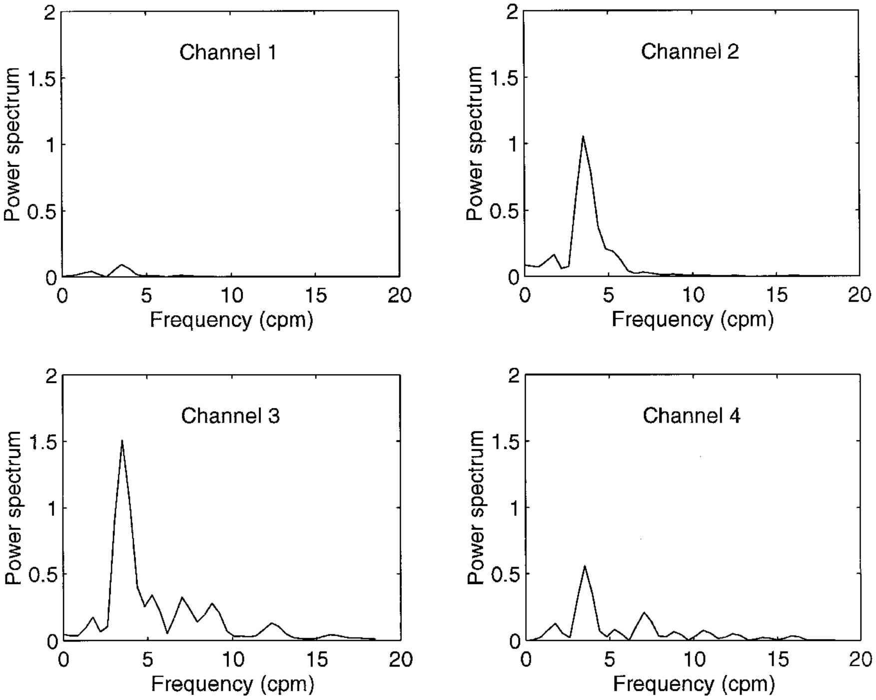

Fig 7. Power spectra of the four-channel EGG signals obtained when the serosal gastric slow waves were coupled. All four-channel EGG signals showed a dominant frequency of 3 cpm. The EGG above the proximal corpus (channel 1) had the lowest power, whereas the EGG above the distal antrum (channel 3) had the highest power.

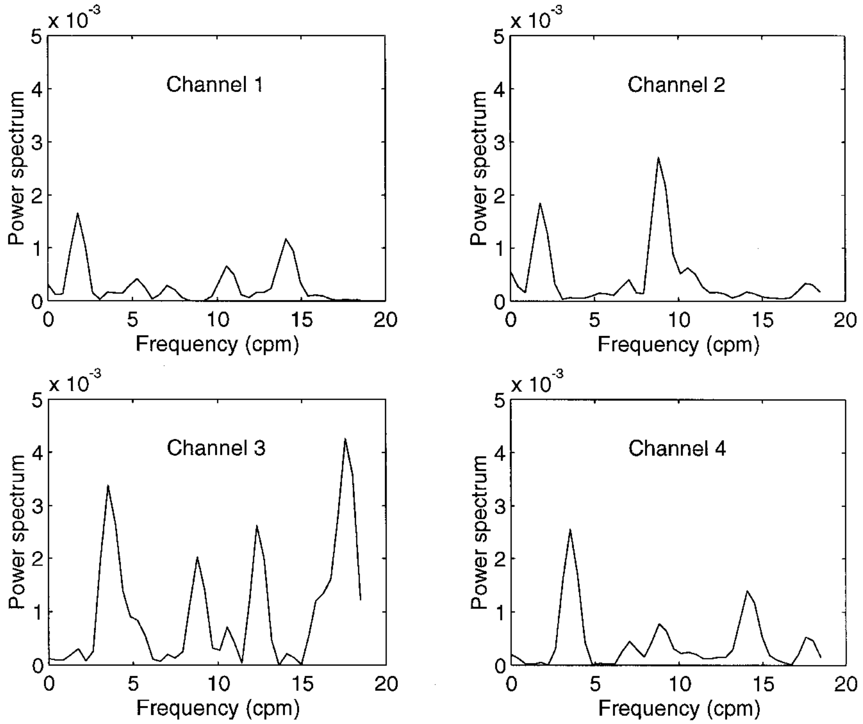

Fig 8. Power spectra of the four-channel EGG signals obtained when the serosal gastric slow waves were completely uncoupled. Under this condition, the different positional EGG signals had totally different power spectra. Channels 1 and 2 showed a combination of bradygastria and tachygastria, channel 3 had a combination of normal 3 cpm and a number of tachygastrias, and channel 4 showed a dominant 3 cpm activity. The absolute power of these four-channel EGG signals was substantially lower than that presented in Figure 6 when the gastric slow waves were coupled. The pattern of the EGG power spectrum in each individual channel varied in different simulations, as shown in Figure 8.

healthy and disease situations to provide guidance for clinical experiments. A few models of GEA have been reported (10, 19, 30–32). A number of different models have been used to simulate the gastric slow waves, including relaxation oscillators (19), Hodgkin-Huxley type oscillators (33), and electric dipoles (10, 19, 30, 31). In this paper, a simple mathematical model was established based on volume conductor theory. The simulation results observed in this paper were in agreement with simulation results by other investigators and/or clinical observations.

When the gastric slow waves are coupled, our simulation results showed that the propagation of the gastric slow wave could be detected from the cutaneous EGGs measured along the antral axis. However, the detectability of the propagation is associated with the observation factor, mainly the thickness of the abdominal wall and the propagation velocity of the slow wave. This is in agreement with the findings presented in one of the previous studies (16). In that previous study, four-channel EGG recordings were made by using four electrodes positioned on the abdomen along the antral axis identified by ultrasonography or x-ray. Phase shifts were observed among different EGG channels in the fasting state in thin volunteers but not in obese volunteers. Forward propagations were observed in a majority of the thin subjects. In another study (34), retrograde propagation of tachygastrial slow waves was observed in a number of patients with gastroparesis. The computer simulations performed by Kothapalli using a three-dimensional model also predicted that the propagation of the gastric slow wave may be detected from the phase shift between different positional EGG signals (32).

Our simulation results have revealed that the amplitude of the EGG is associated with at least the following three factors: the position of the surface electrodes, the coupling/uncoupling of the gastric slow wave, and the propagation velocity of the gastric slow wave. It was found that the EGG measured from the electrodes above the distal antrum had the high-

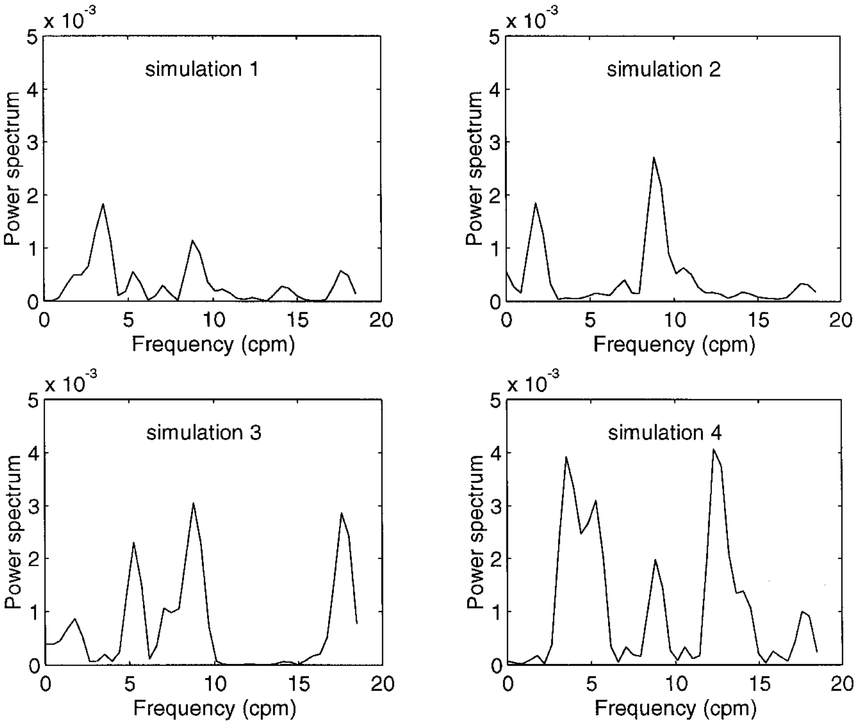

Fig 9. Power spectra of the EGG in Channel 2 obtained in different simulations under the condition that the serosal gastric slow waves were uncoupled. The pattern of the EGG power spectrum was unpredictable and varied in different simulations. Different dominant frequencies were observed in different simulations.

est signal strength. This is in agreement with the findings of Mirizzi and Scafoglieri (35). Although the gastric slow wave may be measured from any site of the body, the signal-to-noise ratio of the EGG measured outside the epigastric area would be substantially low, and the accuracy of the analysis of the EGG would be decreased. Comparing the power spectrum presented in Figures 7 and 8, we can see that the power of the EGG was substantially lower when the gastric slow wave was uncoupled. This has not been reported previously by other investigators but is intuitively understandable. According to the mathematical model presented in this paper, we know that the surface EGG is a weighted summation of all serosal gastric slow waves. The amplitude of the EGG is decreased when the serosal gastric slow waves are not coupled and have random phases. The decrease results from the cancellation of the slow wave amplitudes due to their random phases. Interestingly, our simulation results have shown that the amplitude of the EGG is also associated with the propagation velocity of the gastric slow wave. An increase in the propagation velocity of the gastric slow wave resulted in an increase in the amplitude of the EGG. This is in agreement with a recent study by Familoni et al (31). Using 22 dipoles as a model of GEA, they observed that the amplitude of the EGG was associated with the propagation velocity of the serosal gastric slow wave. However, they did not report whether the total energy of the EGG (the area under the curve) remained unchanged with different propagation velocities. A significantly lower propagation velocity of the gastric slow wave in patients with gastroparesis was previously reported (25). Our data suggest that the amplitude of the EGG is informative of the propagation and coupling of the serosal gastric slow waves. The retrieval of this important and useful information from the amplitude of the EGG is difficult, however, because other factors not related to the gastric slow wave also affect the amplitude of the EGG, such as the skin-electrode impedance, the thickness of the abdominal wall, etc. More efforts have to be made before the absolute value of the EGG amplitude can be used to accurately reflect the characteristics of the gastric slow waves.

In addition to the possibility of the detection of the propagation of the gastric slow wave, multichannel EGG recordings may also be able to reveal the uncoupling of the gastric slow waves, as indicated by our simulation results. In this paper, we have shown that different positional EGG signals had similar power spectra when the serosal gastric slow waves were coupled. The power spectra of the EGG signals at different locations became unpredictable and had different patterns when the serosal gastric slow waves were uncoupled. This is in agreement with recent experimental data determined by Mintchev and Bowes (14). In dogs, they cut the antrum circumferentially to establish a model of uncoupling and observed similar dysrhythmias including tachygastria, bradygastria, and arrhythmia.

Traditionally, it is believed that dysrhythmias in the EGG are caused by similar dysrhythmias of the serosal gastric slow wave. In this paper, however, we have shown that uncoupled gastric slow waves of 3 cpm may generate tachygastria, bradygastria, and arrhythmia. It can be proven mathematically that the weighted summation of 3 cpm nonsinusoidal slow waves with random phases may generate different signals with different frequencies.

In summary, a mathematical model has been established using the volume conductor theory. This model can be used to simulate the transfer of the gastric slow wave from the stomach to the abdominal surface. Different conditions may be simulated using this model. The simulation results of this paper have shown that more information can be retrieved from multichannel EGG recordings than a single-channel EGG recording. The propagation of the gastric slow wave may be detected from the multichannel EGG recordings. The detectability of the propagation is, however, affected by some factors, such as the thickness of the abdominal wall and the propagation velocity of the gastric slow wave. The amplitude of the EGG is associated with the coupling or uncoupling and the propagation velocity of the gastric slow wave. A low amplitude in the EGG may reflect uncoupling or slow propagation of the gastric slow wave. A substantial difference observed in the power spectra of different positional EGG signals is indicative of the uncoupling of the gastric slow wave. The uncoupling of the gastric slow wave may also be reflected in the EGG as dysrhythmias, such as tachygastria, bradygastria, and arrhythmia.

ACKNOWLEDGMENTS

This work was supported by a grant from Teledyne Electronic Technologies under the Teledyne Research Assistant Program. The authors would also like to thank Regina Randall for her preparation of the manuscript.

REFERENCES

1. Alvarez WC: The electrogastrogram and what it shows. JAMA 78:1116–1118, 1992
2. Abell TL, Malagelada J-R: Electrogastrography: Current assessments and future perspective. Dig Dis Sci 83:806–811, 1988
3. Chen J, Pan J, McCallum RW: Clinical significance of gastric myoelectrical dysrhythmias. Dig Dis 13:275–290, 1995
4. Chen J, McCallum RW: Clinical applications of electrogastrogram. Am J Gastroenterol 88:1324–1336, 1993
5. Dubois A: Gastric dysrhythmias: Pathophysiological and etiologic factors. Mayo Clin Proc 64:246–250, 1989
6. Geldof H, van der Schee EJ, Van Blankenstein M, Grashius JL: Electrogastrographic study of gastric myoelectrical activity in patients with unexplained nausea and vomiting. Gut 26:799–808, 1986
7. Kim CH, Zinsmeister AR, Malagelada JR: Effect of gastric dysrhythmias on postcibal motor activity of the stomach. Dig Dis Sci 33:193–199, 1988
8. Koch KL: Gastric dysrhythmias and the current status of electrogastrography. Pract Gastroenterol 13(4):37–44, 1989
9. Stern RM, Koch KL, Stewart WR, Vasey MW: Electrogastrography: Current issues in validation and methodology. Psychophysiol 24:55–64, 1987
10. Smout AJPM, van der Schee EJ, Grashuis JL: What is measured in electrogastrography? Dig Dis Sci 25:179–187, 1980
11. Familoni BO, Bowes KL, Kingma YJ, Cote KR: Can transcutaneous recordings detect gastric electrical abnormalities? Gut 32:141–146, 1991
12. Chen J, Schirmer BD, McCallum RW: Serosal and cutaneous recordings of gastric myoelectrical activity in patients with gastroparesis. Am J Physiol 266:G90–G98, 1994
13. El-Sharkawy TY, et al: Intracellular electrical activity of canine and human gastric smooth muscle. J Physiol 279:291–307, 1978
14. Mintchev MP, Bowes KL: Do increased electrogastrogram frequencies always correspond to internal tachygastria? Ann Biomed Eng (in press)
15. Desvarannes SB, Mizrahi M, Dubois A: Relation between postprandial gastric emptying and cutaneous electrogastrogram in primates. Am J Physiol 261:G248–G255, 1991
16. Chen J, Vandewalle J, Sansen W, van Cutsen E, Vantrappen G, Janssens J: Observation of the propagation direction of human electrogastric activity from cutaneous recordings. Med Biol Eng Comput 27:538–542, 1989
17. Daniel EE: Electrical and contractile activity of pyloric region in dogs and effects of drugs administered intra-arterially. Gastroenterology 49:403–418, 1965
18. Kelly K, Code CF: Effect of transthoracic vagotomy on canine electrical activity. Gastroenterology 55:51–58, 1969
19. Sarna SK: Simulation of the electrical control activity of the stomach by an array of relaxation oscillations. Dig Dis 17:299–310, 1972
20. Koch KL, Stern RM: The relationship between the cutaneously recorded electrogastrogram and antral contractions in man. *In* Electrogastrography. RM Stern, KL Koch (eds). New York, Praeger, 1985, pp 116–131

21. Plonsey R, Fleming D: Bioelectric Phenomena. New York, McGraw-Hill, 1969
22. Schuwan HP, Kay CF: The conductivity of living tissues. Ann NY Acad Sci 65:1007, 1957
23. Plonsey R, Collin R: Principles and Applications of Electromagnetic Fields. New York, McGraw-Hill, 1961
24. Rush S, et al: Resistivity of body tissues at low frequencies. Circ Res 12:40, 1963
25. Chen J, Yi XB, Schirmer BD, Schmieg R, McCallum RW: Impaired propagation of gastric slow waves in gastroparesis and the postoperative period. Gastroenterology 106:A477, 1994
26. Chen J, McCallum RW (eds): Electrogastrography: Principles and Applications. New York, Raven Press, 1994
27. Cucchiara S, Minella R, Riezzo G, Vallone G, Vallone P, Castellone F, Auricchio S: Reversal of gastric electrical dysrhythmias by cisapride in children with functional dyspepsia. Dig Dis Sci 37:1136–1140, 1992
28. Geldof H, van der Schee EJ, Grashuis JL: Electrogastrographic characteristics of interdigestive migrating complex in humans. Am J Physiol 250:G165–G171, 1986
29. Chen J, Lin ZY, Pan J, McCallum RW: Abnormal gastric myoelectrical activity and delayed gastric emptying in patients with symptoms suggestive of gastroparesis. Dig Dis Sci 41(8):1538–1545, 1996
30. Mirizzi N, Stella R, Scafoglieri U: A model of extracellular waveshapes of gastric electrical activity. Med Biol Eng Comput 23:33–37, 1985
31. Familoni BO, Abell TL, Bowes KL: A model of gastric electrical activity in health and disease. IEEE Trans on Biomed Eng 42(7):647–657, 1995
32. Kothapalli B: Electrogastrogram simulation using a three-dimensional model. Med Biol Eng Comp 31(5):482–486, 1993
33. Linkens DA: Electronic modeling of slow-waves and spike-activity in intestinal tissue. IEEE Trans Biomed Eng 27(7):351–357, 1980
34. Chen J, McCallum RW: Electrogastrogram: Measurement, analysis and prospective applications. Med Biol Eng Comput 29:339–350, 1991
35. Mirizzi N, Scafoglieri U: Optimal direction of the electrogastrographic signal in man. Med Biol Eng Comput 21:385–389, 1983